



# Magnesium Nanoparticles With Pd Decoration for Hydrogen Storage

Yana Liu<sup>1,2</sup>, Jinglian Zhu<sup>1,2</sup>, Zhibing Liu<sup>1,2</sup>, Yunfeng Zhu<sup>1,2\*</sup>, Jiguang Zhang<sup>1,2</sup> and Liqun Li<sup>1,2</sup>

<sup>1</sup> College of Materials Science and Engineering, Nanjing Tech University, Nanjing, China, <sup>2</sup> Jiangsu Collaborative Innovation Centre for Advanced Inorganic Function Composites, Nanjing Tech University, Nanjing, China

In this work, Magnesium nanoparticles with Pd decoration, ranging from 40 to 70 nm, were successfully coprecipitated from tetrahydrofuran (THF) solution, assigned as the Mg–Pd nanocomposite. The Mg–Pd nanocomposite exhibits superior hydrogen storage properties. For the hydrogenated Mg–Pd nanocomposite at 150°C, the onset dehydrogenation temperature is significantly reduced to 216.8°C, with a lower apparent activation energy for dehydrogenation of 93.8 kJ/mol H<sub>2</sub>. High-content  $\gamma$ -MgH<sub>2</sub> formed during the hydrogenation process, along with PH<sub>0.706</sub>, contributes to the enhancing of desorption kinetics. The Mg–Pd nanocomposite can take up 3.0 wt% hydrogen in 2 h at a temperature as low as 50°C. During lower hydrogenation temperatures, Pd can dissociate hydrogen and create a hydrogen diffusion pathway for the Mg nanoparticles, leading to the decrease of the hydrogenation apparent activation energy (44.3 kJ/mol H<sub>2</sub>). In addition, the Mg–Pd alloy formed during the hydrogenation/dehydrogenation process can play an active role in the reversible metal hydride transformation, destabilizing the MgH<sub>2</sub>.

**Keywords:** Mg-based nanoparticles, coprecipitation, hydrogen storage,  $\gamma$ -MgH<sub>2</sub> phase, Pd decoration

## OPEN ACCESS

### Edited by:

Zhenguang Huang,  
University of Technology  
Sydney, Australia

### Reviewed by:

Xuezhong Xiao,  
Zhejiang University, China  
Jianfeng Mao,  
University of Wollongong, Australia

### \*Correspondence:

Yunfeng Zhu  
yfzhu@njtech.edu.cn

### Specialty section:

This article was submitted to  
Electrochemistry,  
a section of the journal  
Frontiers in Chemistry

**Received:** 18 November 2019

**Accepted:** 31 December 2019

**Published:** 19 February 2020

### Citation:

Liu Y, Zhu J, Liu Z, Zhu Y, Zhang J and Li L (2020) Magnesium Nanoparticles With Pd Decoration for Hydrogen Storage. *Front. Chem.* 7:949. doi: 10.3389/fchem.2019.00949

## INTRODUCTION

Magnesium hydride has been favorable to be applied foreground in onboard hydrogen storage systems, due to its high gravimetric hydrogen storage capacity (7.6 wt%), natural abundance, and good reversibility. Unfortunately, pure MgH<sub>2</sub> shows slow sorption kinetics and high thermodynamic stability regarding the covered surface oxide layer and the low diffusion coefficient for H (Pistidda et al., 2014; Crivello et al., 2016; Yartys et al., 2019). In order to overcome these drawbacks of MgH<sub>2</sub> for practical applications, numerous studies attempted to enhance the hydrogen storage performance of MgH<sub>2</sub>, such by as alloying Mg with other elements to alter the thermodynamic stability, doping with additives or catalysts, and reducing Mg particles to nano scale. “Nanosize effect” has been considered as an approach with the potential of leading to improvements in both kinetics and thermodynamics (Schneemann et al., 2018), which is based on (i) a larger surface area and thus more hydrogen dissociation sites (ii) the shortened hydrogen diffusion distances which in turn enhance kinetics, and (iii) the increased number of atoms at grain boundaries to enhance the hydrogen diffusion rates (Yao et al., 2011; Schneemann et al., 2018; Sun et al., 2018). Recently, an adapted Rieke method has emerged as an alternative to synthesize Mg nanoparticles to dramatically enhance the hydrogen sorption kinetics of Mg. For instance, Jeon et al. (2011) reported the synthesis of air-stable Mg nanoparticles (~4.9 nm) embedded in PMMA matrix, which enable both the storage of a high hydrogen capacity and rapid kinetics.

Norberg et al. (2011) prepared Mg nanoparticles with controllable sizes by a similar method, and the ab-/desorption hydrogen kinetics were proven to be dramatically faster for nanoparticles with smaller sizes, as a result of the increase of the defect density formed in smaller nanoparticles. Recently, we have investigated that the Mg-TM (TM = Ni, Ti, Fe, Co, and V) nanocomposites can be coprecipitated from solution, in which the coprecipitated Ni, Ti, Fe, V, or Co has high catalytic efficiency in improvement of the ab-/desorption hydrogen kinetics of Mg nanoparticles (Liu et al., 2014a,b, 2015). The adapted Rieke method is considered as a better method for the preparation of nano-sized Mg with controllable sizes, and which can dope transition metal catalysts into a Mg/MgH<sub>2</sub> system by a simple chemical route. With regard to the nanoscaling, various catalysts for improving the hydrogen storage properties of MgH<sub>2</sub> have been investigated, such as transition metals/metal oxides/halogenides (Ma et al., 2009, 2013; Cui et al., 2014; Rizo-Acosta et al., 2018; Zhang et al., 2018; Liu et al., 2019b), rare earth metal oxides/halogenides (Singh et al., 2013; Lin et al., 2014, 2015; Wang et al., 2015), carbon materials (Lukashev et al., 2006; Liu et al., 2013; Rather et al., 2016), and other hydrides (Lu et al., 2010; Terent'ev et al., 2015; Jangir et al., 2018). In addition, some noble metals, such as Pd, have been reported to be effective for facilitating hydrogenation of MgH<sub>2</sub> (Du et al., 2007; Callini et al., 2010; Ham et al., 2013; Chung et al., 2015; Liu et al., 2019a). Liu et al. (2019a) reported that elemental Pd played a dominant role in accelerating the preferential diffusion of hydrogen atoms at the Pd/Mg interface, during the hydrogenation process. Callini et al. (2009) suggested the occurrence of Mg-alloying as a path for subsequent feasible H-exchange, when Pd was deposited on top of a thick MgO layer surrounding the Mg NPs core. Du et al. (2007) reported that the Pd-dopant provides a much lower activation barrier for both dissociation of molecular hydrogen and diffusion of atomic hydrogen on the Mg surface, based on ab initio density functional theory calculations.

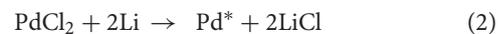
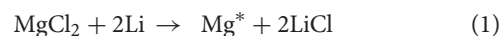
Inspired by the above considerations, a Mg-Pd nanocomposite was coprecipitated from THF solution. The Mg nanoparticles were homogeneously decorated with nano-sized Pd. The hydrogen sorption properties were investigated, and the catalytic mechanisms of Pd were also proposed.

## MATERIALS AND METHODS

### Sample Preparation

As early as in 1972, Rieke et al. reported a general procedure for the preparation of highly reactive magnesium metal, which was prepared by reducing a magnesium halide with alkali metal in an ethereal solvent (Rieke and Hudnall, 1972). In this work, anhydrous MgCl<sub>2</sub>, PdCl<sub>2</sub>, lithium naphthalide (LiNp), and tetrahydrofuran (THF) solution were introduced to prepare the Mg-Pd nanocomposite by the coprecipitation method (an adapted Rieke method). During the sample preparation process, the real reducing agent is metal Li, while naphthalene is used as an electron carrier. Due to the presence of naphthalene, metal Li would dissolve in THF, forming a blackish green solution, which can speed up the reduction reaction of active Mg. In raw materials, Pd:Mg was

kept in a weight ratio of 1:9. The reaction processes are as follows:



Naphthalene (5.52 g) and lithium (0.299 g) were dissolved in the freshly distilled THF (50 ml), forming a homogeneous blackish green solution (LiNp/THF). A mixed THF solution of MgCl<sub>2</sub> and PdCl<sub>2</sub> was prepared by anhydrous MgCl<sub>2</sub> (1.904 g) and PdCl<sub>2</sub> (0.09 g) dissolved in 200 ml THF at 60–70°C. The coprecipitation reaction process and the separation and drying process of nanocomposites were performed with reference to a relevant literature report (Liu et al., 2014b).

### Sample Characterization

The crystal structure and the phase composition of the samples were analyzed by X-ray diffraction (XRD) with Cu K $\alpha$  radiation (40 kV and 35 mA) using an ARL X'TRA diffractometer. The morphology and microstructure of as-prepared samples were observed by using a JEM-2100F transmission electron microscope (TEM). A Sieverts-type apparatus (AMC) was used to examine the hydrogen storage properties. The auto pressure–composition–temperature (PCT) measurements were performed under a hydrogen pressure up to 4 MPa. The hydrogen absorption kinetics was characterized under an initial hydrogen pressure of 3.0 MPa. The dehydrogenation experiments were performed using diffraction scanning calorimetry (DSC, Netzsch STA 449F3) at various heating rates under Ar gas flow.

## RESULTS AND DISCUSSION

### Microstructural Characterization

Figure 1 presents the XRD patterns of the Mg-Pd nanocomposite in varying states. As shown in Figure 1A,

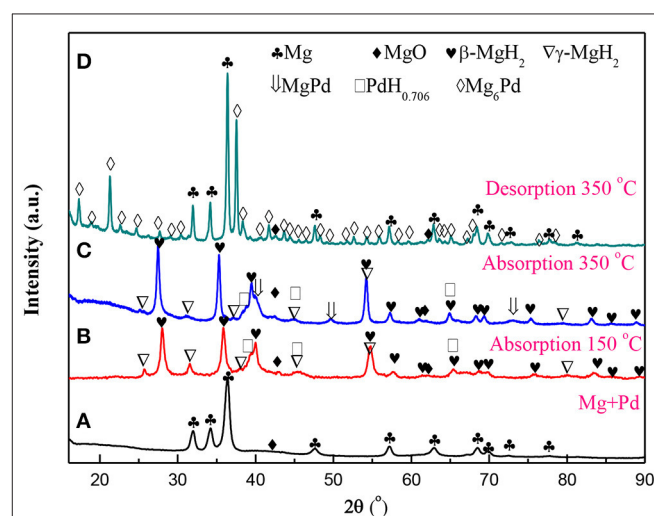


**FIGURE 1** | X-ray diffraction (XRD) patterns for the Mg-Pd nanocomposite in varying states. **(A)** As prepared, **(B,C)** hydrogenated at 150 and 350°C for 2 h, and **(D)** dehydrogenated at 350°C for 2 h.

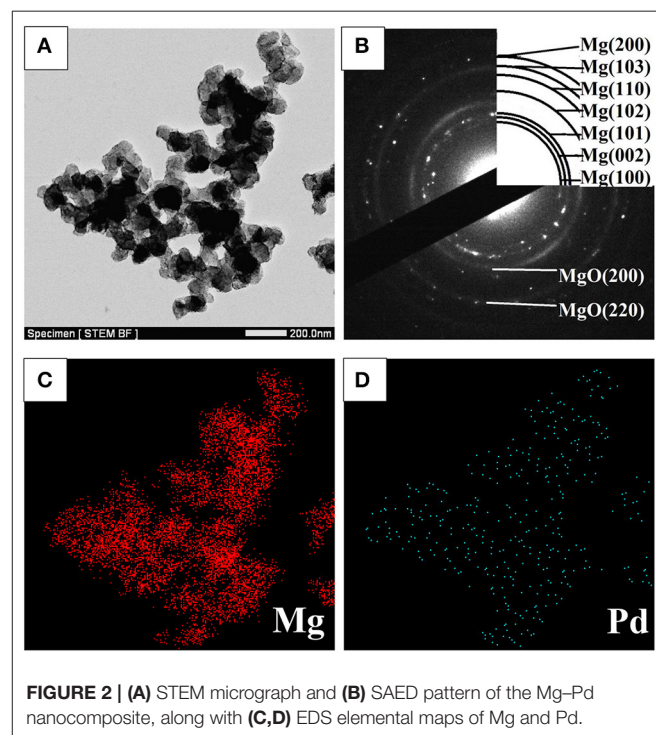
almost all diffraction peaks of as-prepared nanocomposite can be characterized with the hexagonal Mg phase. Only a weak peak at  $\sim 42.9^\circ$  can be indexed with MgO, and the characteristic diffraction peaks of Pd are absent. A small amount of MgO is likely due to the oxidation in the process of sample preparation for the XRD analysis, as a result of high chemical activity of Rieked Mg. The absence of Pd peaks suggests that Pd synthesized from solution is in the form of extremely fine particles or amorphous, and hence, it does not generate detectable diffraction intensity. A similar phenomenon has been found in our previous research work (Liu et al., 2014a, 2015). The lattice parameters of the Mg phase can be refined to be  $a = b = 0.3225$  nm, and  $c = 0.5242$  nm for the Mg-Pd nanocomposite, which are slightly larger than those of pure Mg reduced by the same method ( $a = b = 0.3196$  nm,  $c = 0.5199$  nm; Liu et al., 2014b), indicating that a part of the Pd atoms may get into the crystal lattice of the Mg during the preparation, resulting in the lattice expansion of Mg. In addition, the average crystallite of Mg can be determined to be about 22.5 nm by the Scherrer equation. When the Mg-Pd nanocomposite was hydrogenated under 3 MPa hydrogen pressure at  $150^\circ\text{C}$  for 2 h, the majority phases of the hydrogenated Mg-Pd nanocomposite are the tetragonal  $\beta$ -MgH<sub>2</sub> and the orthogonal  $\gamma$ -MgH<sub>2</sub>, along with a small amount of MgO and PdH<sub>0.706</sub> phases, as shown in **Figure 1B**. The metastable  $\gamma$ -MgH<sub>2</sub>, belonging to a-PbO<sub>2</sub>-type orthorhombic crystal structure, is usually produced by ball milling (Varin et al., 2006; Ponthieu et al., 2013; Zhou et al., 2015) as well as under high compressive stress (Vajeeston et al., 2006; Siviero et al., 2009; Ham et al., 2013). Zhou et al. (2013) pointed out that the H octahedrons surrounding Mg atoms are deformed in the  $\gamma$ -MgH<sub>2</sub>. Besides, the octahedral chain takes a zigzag form, while for the  $\beta$ -MgH<sub>2</sub>, the chain is straight. Sander et al. studied hydrogen transport kinetics in  $\beta$ - (termed  $\alpha$ -MgH<sub>2</sub> in their study) and  $\gamma$ -MgH<sub>2</sub> based on theoretical calculations and found that H vacancies' concentrations are higher and more mobile in the  $\gamma$ -MgH<sub>2</sub> than in the  $\beta$ -MgH<sub>2</sub> (Sander et al., 2016). Therefore, we can speculate that the metastable  $\gamma$ -MgH<sub>2</sub> structure is likely due to the deformations and structural defects formed in the MgH<sub>2</sub> lattice during the preparation (ball milling or under high compressive stress). The formation of the  $\gamma$ -MgH<sub>2</sub> phase is also found in the Mg-TM (TM = Ni, Ti, Fe, Co, and V) nanocomposites coprecipitated from solution (Liu et al., 2014a,b, 2015). Norberg et al. (2011) proposed that a high density of defects may form in the Mg lattice through the adapted Rieked method. In addition, Xiao et al. (2016) synthesized  $\beta$ -/ $\gamma$ -MgH<sub>2</sub> nanocomposites via a simple wet chemical route by ball milling MgH<sub>2</sub> with LiCl as an additive at room temperature followed by THF treatment and revealed that THF solution plays a vital role in the synthesis of the  $\gamma$ -MgH<sub>2</sub> phase. In this work, high-density defects formed in the nanocomposite and THF solution effect may contribute to the formation of the  $\gamma$ -MgH<sub>2</sub> phase at lower temperature. On hydrogen loading, the PdH<sub>0.706</sub> peaked at  $38.7^\circ\text{C}$ , corresponding to the (111) plane. The PdH<sub>0.706</sub> phase also could be found when Au/Mg/Pd films were hydrogenated at  $200^\circ\text{C}$  (Akyildiz et al., 2006). As the temperature was increased to  $350^\circ\text{C}$ , in addition to the main phase of  $\beta$ -MgH<sub>2</sub>, MgPd, PdH<sub>0.706</sub>, and  $\gamma$ -MgH<sub>2</sub> phases were

clearly detected in **Figure 1C**. The appearance of the Pd-rich intermetallic compound MgPd indicates that Pd is inter-mixing with Mg at the Pd-Mg interface, which is considered to be the equilibrium end product (Callini et al., 2010). The amount of  $\gamma$ -MgH<sub>2</sub> phase in hydrogenated nanocomposite decreased with increasing the hydrogenation temperature, due to the removal of the lattice deformation and structural defects in Mg at high temperature. Shena and Aguey-Zinsou, reported that the  $\gamma$ -MgH<sub>2</sub> was fully converted to  $\beta$ -MgH<sub>2</sub> after hydrogen cycling at  $200^\circ\text{C}$ , due to the annealing of defects and relief of strain (Shena and Aguey-Zinsou, 2017). After dehydrogenation at  $350^\circ\text{C}$  for 2 h under 0.05 MPa hydrogen pressure, the phases of Mg, MgO, and Mg<sub>6</sub>Pd could be detected in the XRD pattern of **Figure 1D**. The formation of Mg<sub>6</sub>Pd confirms an interaction between MgH<sub>2</sub> and MgPd or PdH<sub>0.706</sub> during the process of dehydrogenation, as in following equations:



Huot et al. (2009) found that the bulk Mg<sub>6</sub>Pd could reversibly absorb hydrogen in three disproportionation reactions and finally be transformed to the MgPd phase again. MgPd or PdH<sub>0.706</sub> interacting with MgH<sub>2</sub> may alter the thermodynamics of the dehydrogenation of MgH<sub>2</sub>. Therefore, the thermodynamics of the Mg-Pd nanocomposite will be discussed in greater detail later.

STEM micrographs and SAED pattern of the Mg-Pd nanocomposite are shown in **Figure 2**. The Mg-Pd nanocomposite is composed of irregularly shaped particles aggregating together, with their particle sizes ranging from 40



to 70 nm, as shown in **Figure 2A**, while for the pure Mg without doping catalysts, the nanoparticles were plate-shaped and stacked together forming a shape like a “chicken claws” structure (Liu et al., 2014b). The above result indicates that doping with Pd may dramatically affect the preferred orientation of Mg particle growth. As shown in the corresponding SAED pattern (**Figure 2B**), the diffraction rings or points can be indexed with Mg and MgO phase, without Pd, which is in accordance with the XRD result. In order to qualitatively evaluate the distribution of Pd in Mg particles, EDS elemental maps of Mg and Pd were performed. As can be seen, Pd is homogeneously distributed on the surface or inside Mg particles, without obvious reunion phenomenon. The actual Pd weight content in the nanocomposite is about 5 wt%, much lower than the initial doping amount. Only half the amount of Pd was embedded in or attached on the surface of Mg particles, and the rest might be lost during the centrifugation and repeated washing processes. The TEM micrograph and the corresponding SAED pattern of the Mg–Pd nanocomposite hydrogenated at 150°C for 2 h are shown in **Figures 3A,B**, respectively. As can be seen, the particle size of the hydrogenated Mg–Pd nanocomposite ranges from 20 to 30 nm, much lower than that hydrogenated before, which is likely due to a large number of nucleation sites at the Mg–Pd interface and high density of defects on the Mg particles. The same phenomenon was found in the previously reported Mg–TM (TM = Ni, Ti, Fe, Co, and V) nanocomposites (Liu et al., 2014a,b, 2015). As shown in the STEM images, Pd is homogeneously distributed on the surface or inside Mg particles, without obvious reunion phenomenon. Kumar et al. has reported that multinucleation sites for the Mg→MgH<sub>2</sub> hydrogenation process could be created by the uniformly distributed catalyst on the Mg nanoparticle surface, which could prevent grain growth (Kumar et al., 2017). A high density of defects on the Mg particles could also be found in the previously reported Mg–TM (TM = Ni, Ti, Fe, Co, and V) nanocomposites (Liu et al., 2014a,b, 2015) and Mg nanocrystals prepared by Norberg et al. (2011), which could provide more nucleation sites for the Mg→MgH<sub>2</sub> hydrogenation process. In addition, the particles’ growth trend is not obvious at lower hydrogenation temperature (150°C), resulting in the refinement of MgH<sub>2</sub> particles. As shown in **Figure 3B**, no diffraction

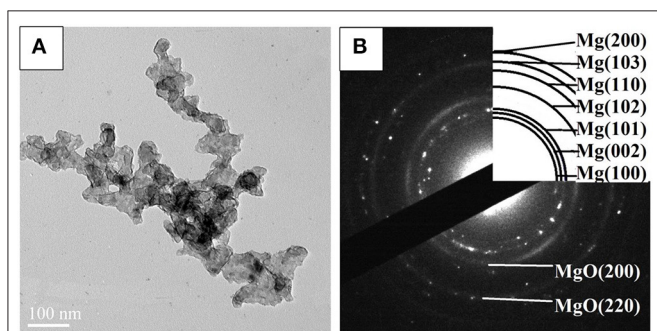


**FIGURE 3 | (A)** Transmission electron microscope (TEM) micrograph and **(B)** SAED pattern of the Mg–Pd nanocomposite hydrogenated at 150°C for 10 h.

rings or points can be indexed with the  $\beta$ -/ $\gamma$ -MgH<sub>2</sub> phase, suggesting that the electron beam induces full dehydrogenation of MgH<sub>2</sub> during the TEM measurement under high-vacuum conditions. Besides, Pd or PdH<sub>0.706</sub> is not found, maybe due to the poor crystallinity.

## The Effects of Mg<sub>6</sub>Pd on the Thermodynamics

**Figure 4A** displays the PCT curves of the Mg–Pd nanocomposite measured at different temperatures in a hydrogen pressure range from 0.02 to 4 MPa. The first hydrogen cycle at 350°C was conducted for the test sample to obtain a Mg–Mg<sub>6</sub>Pd system. It can be found that only one plateau is present across the whole range of the hydrogen content in each PCT curve. Obvious plateaus of Mg<sub>6</sub>Pd cannot be clearly identified. However, previous investigation (Huot et al., 2009) showed that the hydrogen absorption process of Mg<sub>6</sub>Pd was divided into three stages:

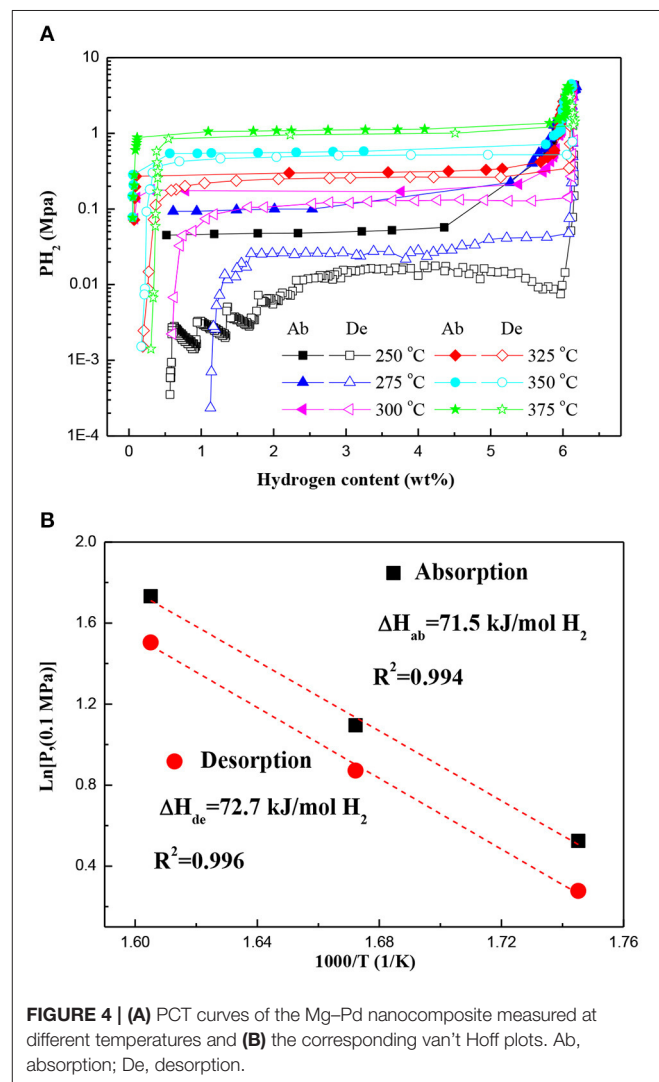
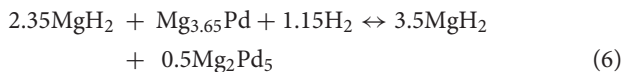


**FIGURE 4 | (A)** PCT curves of the Mg–Pd nanocomposite measured at different temperatures and **(B)** the corresponding van't Hoff plots. Ab, absorption; De, desorption.

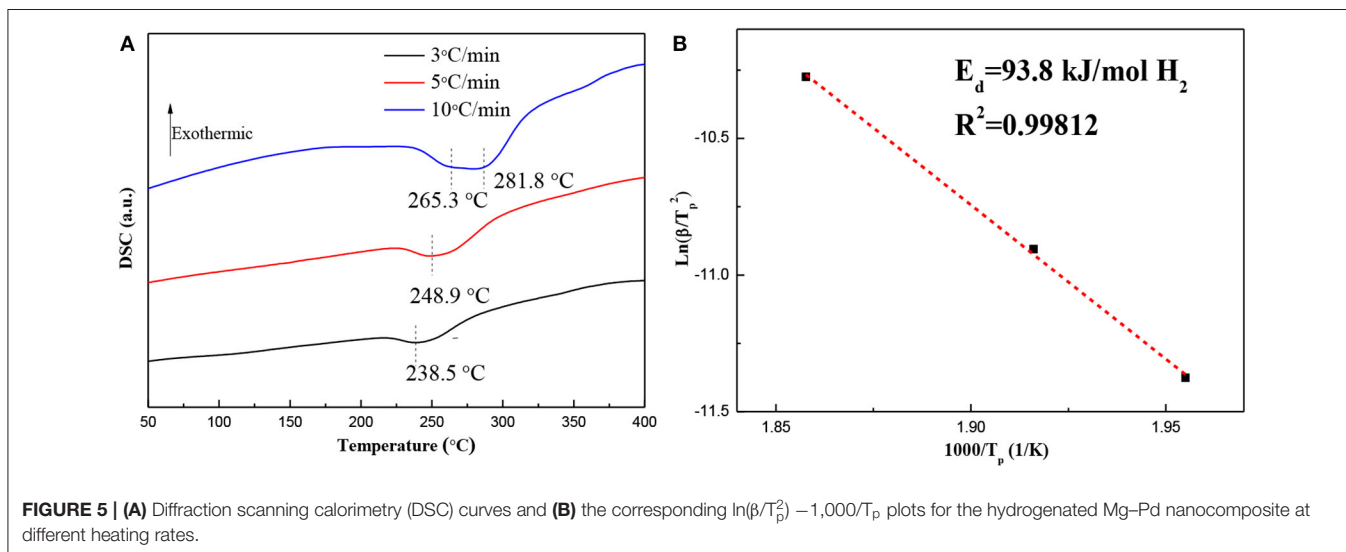


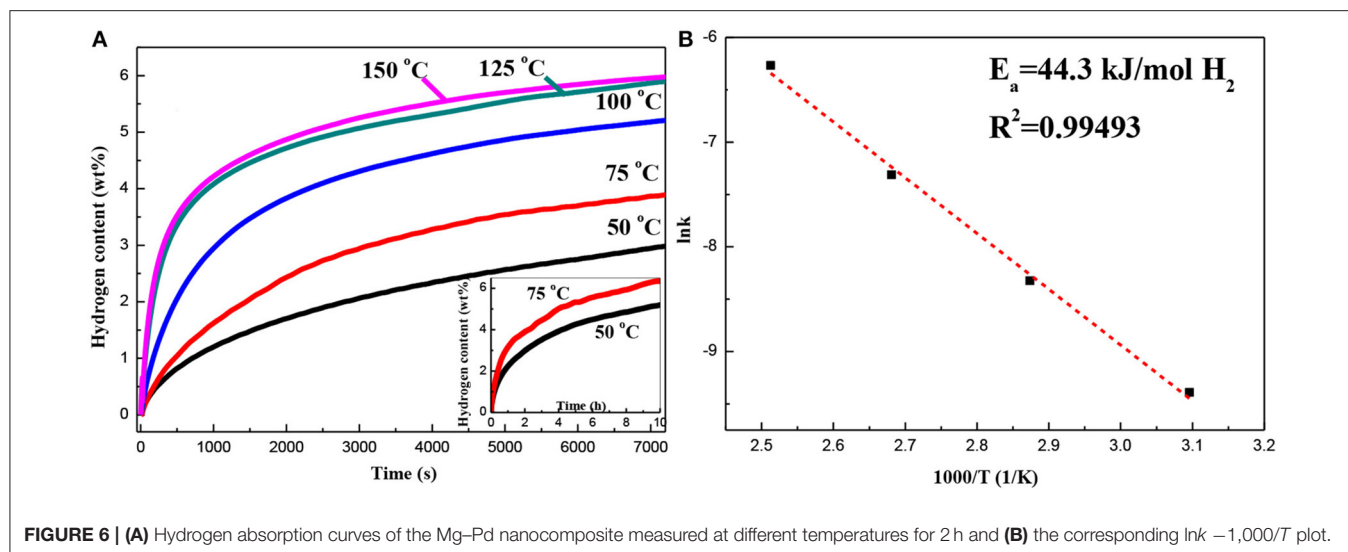
A higher plateau should appear in the PCT curve, which is attributed to the transformation  $\text{Mg}_6\text{Pd} + 5\text{H}_2 \leftrightarrow \text{MgPd} + 5\text{MgH}_2$ . In addition, Shena and Aguey-Zinsou (2017) reported that  $P(\text{H}_2)_{\text{abs}} = 5 \text{ MPa}$  is not sufficient to induce the formation of MgPd at the higher temperature of 350°C. In fact, at 350°C, 3 MPa is enough for the formation of MgPd, as shown in **Figure 1C**. This is in accordance with the one plateau observed in the PCT curve for the Mg–Mg<sub>6</sub>Pd system, suggesting an excellent synergistic effect for Mg and Mg<sub>6</sub>Pd during hydrogenation/dehydrogenation processes. The corresponding van't Hoff plot ( $\ln P$  vs.  $1/T$ ) is used to estimate hydrogenation and dehydrogenation enthalpies, as shown in **Figure 4B**. The hydrogenation and dehydrogenation enthalpies are determined to be  $-71.5$  and  $72.7 \text{ kJ mol}^{-1} \text{ H}_2$ , respectively, which are slightly lower than that of pristine MgH<sub>2</sub> ( $74.7 \text{ kJ mol}^{-1} \text{ H}_2$ ; Crivello et al., 2016). Zhang et al. found that MgH<sub>2</sub> is preferentially decomposed by virtue of the Mg–Pd alloy instead of self-decomposition, which can reduce thermal stability of the MgH<sub>2</sub> through interacting with MgH<sub>2</sub> and forming the Mg<sub>6</sub>Pd phase (Zhang et al., 2015). Therefore, it is reasonable to suggest that the Mg–Pd alloy plays an active role in the reversible metal hydride transformation, destabilizing the MgH<sub>2</sub>.

### The Effects of $\gamma$ -MgH<sub>2</sub> and PdH<sub>0.706</sub> on Dehydrogenation Performances

DSC curves and the corresponding  $\ln(\beta/T_p^2) - 1,000/T_p$  plots for the hydrogenated Mg–Pd nanocomposite are shown in **Figure 5**. The Mg–Pd nanocomposite was hydrogenated at 150°C for 2 h, as the test sample. **Figure 5A** shows that there is a broader and asymmetrical endothermic peak corresponding to desorption of the  $\gamma$ -MgH<sub>2</sub> and  $\beta$ -MgH<sub>2</sub> phases in 238.5 and 248.9°C at

heating rates of 3 and 5°C/min, respectively, while for the heating rates of 10°C/min, the final endothermic peak is a superposition of two contributing peaks of 265.3 and 281.8°C. The above results suggest that  $\gamma$ -MgH<sub>2</sub> decomposes along with the  $\beta$ -MgH<sub>2</sub>, which may trigger the decomposition of the  $\beta$ -MgH<sub>2</sub> during the dehydrogenation process. The onset dehydrogenation temperature at a heating rate of 3°C/min is reduced to 216.8°C, representing a 94.3°C reduction as compared with the pure MgH<sub>2</sub> prepared through the same method (Liu et al., 2014b), and for the reported Mg–TM (TM = Ni, Ti, Fe, Co, and V) nanocomposites, the onset dehydrogenation temperatures were determined to be 244.6, 296.1, 246.5, 249.1, and 278.2°C, respectively (Liu et al., 2014a,b, 2015). The hydrogenated Mg–Pd nanocomposite exhibits superior hydrogen desorption kinetics compared with the previously reported Mg–TM (TM = Ni, Ti, Fe, Co, and V) nanocomposites. The pure MgH<sub>2</sub> is a single phase of  $\beta$ -MgH<sub>2</sub>, without doping catalyst. The  $\gamma$ -MgH<sub>2</sub> phase is known to be less stable than the  $\beta$ -MgH<sub>2</sub> phase. The plane (110) of  $\gamma$ -MgH<sub>2</sub> has a predicted enthalpy of  $44.66 \text{ kJ mol}^{-1} \text{ H}_2$ , while for the same  $\beta$ -MgH<sub>2</sub> plane, the enthalpy is  $78.16 \text{ kJ mol}^{-1} \text{ H}_2$  (Zhou et al., 2015). In addition, the heavily distorted MgH<sub>6</sub> octahedron in the  $\gamma$ -MgH<sub>2</sub> potentially can facilitate hydrogen diffusion (Sander et al., 2016). Shena and Aguey-Zinsou (2017) proposed that  $\gamma$ -MgH<sub>2</sub> can further facilitate hydrogen desorption from  $\beta$ -MgH<sub>2</sub>, which can act as a pathway for faster hydrogen diffusion. In this work, a higher content of  $\gamma$ -MgH<sub>2</sub> is achieved in the hydrogenated products, as shown in **Figure 1B**. Therefore, it can be concluded that the  $\gamma$ -MgH<sub>2</sub> phase can significantly reduce the dehydrogenation temperature and improve the dehydrogenation kinetics by acting as a pathway for faster hydrogen diffusion. The PdH<sub>0.706</sub> phase in the hydrogenated products also is reported to be effective for improving desorption hydrogen kinetics and reducing the hydrogen desorption temperature, which may help the recombination process of H atoms into hydrogen molecules on the surface (Tang et al., 2008). Higuchi et al. (2002) reported that “cooperative phenomena”





can explain the significant improvement in the dehydrogenating properties of the Pd/Mg/Pd films, in which hydrogen exhibits elastic interactions between  $\text{MgH}_2$  and  $\text{PdH}_{0.6}$ . The activation energy,  $E_d$ , for the hydrogen desorption mechanism of the hydrogenated Mg-Pd nanocomposites is estimated by the Kissinger equation:

$$\ln(\beta/T_p^2) = A - E_d/(RT_p) \quad (8)$$

where  $\beta$  is the heating rate,  $T_p$  is the peak temperature, and A is a linear constant.

**Figure 5B** shows the plot of  $\ln(\beta/T_p^2)$  vs.  $1,000/T_p$  for the hydrogenated Mg-Pd nanocomposites. The  $E_d$  value can be determined to be 93.8 kJ/mol  $\text{H}_2$ , which is much lower than that of the hydrogenated pure Mg (147.4 kJ/mol  $\text{H}_2$ ; Liu et al., 2014b) and the reported Mg-TM (TM = Ni, Ti, Fe, Co, and V) nanocomposites (139.1, 170.9, 118.1, 110.1, and 147.7 kJ/mol  $\text{H}_2$ , respectively; Liu et al., 2014a,b, 2015). The lower dehydrogenation temperature and  $E_d$  value indicate that  $\gamma\text{-MgH}_2$  and  $\text{PH}_{0.706}$  phases formed during the hydrogenation process contribute to the enhancing desorption kinetics.

## The Effects of Pd on Lower Temperature Hydrogenation Performances

**Figure 6A** shows the first isothermal hydrogen absorption curves of the Mg-Pd nanocomposite measured at 50, 75, 100, 125, and 150°C. As can be seen, the Mg-Pd nanocomposite exhibits excellent hydrogen absorption performance. The hydrogen storage capacity can reach up to 3.0 wt% in 2 h at 50°C. In contrast, the hydrogen capacity of the pure Mg is 2.6 wt% within 2 h at a higher temperature of 125°C. The result suggests that Pd exhibits high catalytic activity on accelerating the hydrogenation rate of Mg. The apparent activation energy of dehydrogenation can be calculated based on the Johnson-Mehl-Avrami-Kolmogorov (JMAK) model and the Arrhenius

theory (Liu et al., 2014a,b, 2015). The Arrhenius-type plot of  $\ln k$  vs.  $1,000/T$  is drawn in **Figure 6B**. Thus,  $E_a$  of the Mg-Pd nanocomposite can be determined to be 44.3 kJ/mol  $\text{H}_2$ , much lower than that of the pure Mg (73.1 kJ/mol  $\text{H}_2$ ; Liu et al., 2014b). Such a low energy barrier explains the excellent absorption kinetics of the Mg-Pd nanocomposite at low temperatures. As shown in the STEM images (**Figure 2**), Pd is homogeneously distributed on the surface or inside Mg particles, with the particle size ranging from 40 to 70 nm. The reported theoretical calculations indicate that the Pd-dopant can provide a much lower activation barrier for both dissociation of molecular hydrogen and diffusion of atomic hydrogen on the Mg surface (Du et al., 2007). Pd in the form of small particles dispersed on the Mg particles can catalyze the dissociation of  $\text{H}_2$ , and the adsorbed hydrogen atoms can be spilled over onto the surface of Mg nanoparticles, which is assigned as a “spillover” mechanism (Zaluska et al., 1995). In addition, Pd may act as the “nanoportal” role, and hydride nucleation occurs only under Pd nanoparticles at lower hydrogenation temperature (Chung et al., 2015). Hence, it can be concluded that Pd homogeneously distributed on the surface or inside Mg particles can dissociate hydrogen and create a hydrogen diffusion pathway for the Mg nanoparticles.

## CONCLUSIONS

In this work, a Mg-Pd nanocomposite was successfully coprecipitated from a homogeneous THF solution. STEM observations revealed that Pd was homogeneously distributed on the surface or inside Mg particles, with the particle size ranging from 40 to 70 nm. The Mg-Pd nanocomposite exhibits superior hydrogen storage properties. The hydrogen reaction enthalpies of the Mg-Pd nanocomposite are slightly lower than that of pristine  $\text{MgH}_2$ , indicating that the Mg-Pd alloy plays an active role in the reversible metal hydride

transformation and destabilizes the MgH<sub>2</sub>. For the hydrogenated Mg-Pd nanocomposite at 150°C, the onset dehydrogenation temperature is reduced to 216.8°C, representing a 94.3°C reduction as compared with the pure MgH<sub>2</sub> prepared through the same method. High-content  $\gamma$ -MgH<sub>2</sub> along with PH<sub>0.706</sub> is formed during the hydrogenation process, contributing to the enhancing desorption kinetics. The Mg-Pd nanocomposite can take up 3.0 wt% hydrogen in 2 h at temperature low as 50°C. During lower hydrogenation temperatures, Pd can dissociate hydrogen and create a hydrogen diffusion pathway for the Mg nanoparticles.

## DATA AVAILABILITY STATEMENT

All datasets generated for this study are included in the article/supplementary material.

## REFERENCES

- Akyildiz, H., Ozenbas, M., and Ozturk, T. (2006). Hydrogen absorption in magnesium based crystalline thin films. *Int. J. Hydr. Energy* 31, 1379–1383. doi: 10.1016/j.ijhydene.2005.11.003
- Callini, E., Pasquini, L., Piscopiello, E., Montone, A., Vittori Antisari, M., and Bonetti, E. (2009). Hydrogen sorption in Pd-decorated Mg-MgO core-shell nanoparticles. *Appl. Phys. Lett.* 94:221905. doi: 10.1063/1.3147205
- Callini, E., Pasquini, L., Rude, L. H., Nielsen, T. K., Jensen, T. R., and Bonetti, E. (2010). Hydrogen storage and phase transformations in Mg-Pd nanoparticles. *J. Appl. Phys.* 108:073513. doi: 10.1063/1.3490206
- Chung, C. J., Nivargi, C., and Clemens, B. (2015). Nanometer-scale hydrogen 'portals' for the control of magnesium hydride formation. *Phys. Chem. Chem. Phys.* 17, 28977–28984. doi: 10.1039/C5CP04515K
- Crivello, J. C., Dam, B., Denys, R. V., Dornheim, M., Grant, D. M., Huot, J., et al. (2016). Review of magnesium hydride-based materials: development and optimisation. *Appl. Phys. A* 122:97. doi: 10.1007/s00339-016-9602-0
- Cui, J., Liu, J., Wang, H., Ouyang, L., Sun, D., Zhu, M., et al. (2014). Mg-TM (TM: Ti, Nb, V, Co, Mo or Ni) core-shell like nanostructures: synthesis, hydrogen storage performance and catalytic mechanism. *J. Mater. Chem. A* 2, 9645–9655. doi: 10.1039/C4TA00221K
- Du, A. J., Smith, S. C., Yao, X. D., and Lu, G. Q. (2007). Hydrogen spillover mechanism on a Pd-doped Mg surface as revealed by ab initio density functional calculation. *J. Am. Chem. Soc.* 129, 10201–10204. doi: 10.1021/ja0722776
- Ham, B., Junkaew, A., Arroyave, R., Chen, J., Wang, H., Wang, P., et al. (2013). Hydrogen sorption in orthorhombic Mg hydride at ultra-low temperature. *Int. J. Hydr. Energy* 38, 8328–8341. doi: 10.1016/j.ijhydene.2013.04.098
- Higuchi, K., Yamamoto, K., Kajioka, H., Toiyama, K., Honda, M., Orimoc, S., et al. (2002). Remarkable hydrogen storage properties in three-layered Pd/Mg/Pd thin films. *J. Alloys Comp.* 330, 526–530. doi: 10.1016/S0925-8388(01)01542-0
- Huot, J., Yonkeu, A., and Dufour, J. (2009). Rietveld analysis of neutron powder diffraction of Mg6Pd alloy at various hydriding stages. *J. Alloys Comp.* 475, 168–172. doi: 10.1016/j.jallcom.2008.07.034
- Jangir, M., Jain, A., Agarwal, S., Zhang, T., Kumar, S., Selvaraj, S., et al. (2018). The enhanced de/re-hydrogenation performance of MgH<sub>2</sub> with TiH<sub>2</sub> additive. *Int. J. Energy Res.* 42, 1139–1147. doi: 10.1002/er.3911
- Jeon, K. J., Moon, H. R., Ruminski, A. M., Jiang, B., Kisielowski, C., Bardhan, R., et al. (2011). Air-stable magnesium nanocomposites provide rapid and high-capacity hydrogen storage without using heavy-metal catalysts. *Nat. Mater.* 10, 286–290. doi: 10.1038/nmat2978
- Kumar, S., Jain, A., Yamaguchi, S., Miyaoka, H., Ichikawa, T., Mukherjee, A., et al. (2017). Surface modification of MgH<sub>2</sub> by ZrCl<sub>4</sub> to tailor the reversible hydrogen storage performance. *Int. J. Hydr. Energy* 42, 6152–6159. doi: 10.1016/j.ijhydene.2017.01.193
- Lin, H.-J., Matsuda, J., Li, H.-W., Zhu, M., and Akiba, E. (2015). Enhanced hydrogen desorption property of MgH<sub>2</sub> with the addition of cerium fluorides. *J. Alloys Comp.* 645, S392–S396. doi: 10.1016/j.jallcom.2014.12.102
- Lin, H.-J., Tang, J.-J., Yu, Q., Wang, H., Ouyang, L.-Z., Zhao, Y.-J., et al. (2014). Symbiotic CeH 2.73/CeO<sub>2</sub> catalyst: a novel hydrogen pump. *Nano Energy* 9, 80–87. doi: 10.1016/j.nanoen.2014.06.026
- Liu, G., Wang, Y., Xu, C., Qiu, F., An, C., Li, L., et al. (2013). Excellent catalytic effects of highly crumpled graphene nanosheets on hydrogenation/dehydrogenation of magnesium hydride. *Nanoscale* 5, 1074–1081. doi: 10.1039/C2NR33347C
- Liu, M., Xiao, X., Zhao, S., Chen, M., Mao, J., Luo, B., et al. (2019a). Facile synthesis of Co/Pd supported by few-walled carbon nanotubes as an efficient bidirectional catalyst for improving the low temperature hydrogen storage properties of magnesium hydride. *J. Mater. Chem. A* 7, 5277–5287. doi: 10.1039/C8TA12431K
- Liu, M., Xiao, X., Zhao, S., Saremi-Yarhamadi, S., Chen, M., Zheng, J., et al. (2019b). ZIF-67 derived Co@CNTs nanoparticles: remarkably improved hydrogen storage properties of MgH<sub>2</sub> and synergetic catalysis mechanism. *Int. J. Hydr. Energy* 44, 1059–1069. doi: 10.1016/j.ijhydene.2018.11.078
- Liu, Y., Zou, J., Zeng, X., and Ding, W. (2014a). A co-precipitated Mg-Ti nano-composite with high capacity and rapid hydrogen absorption kinetics at room temperature. *RSC Adv.* 4, 42764–42771. doi: 10.1039/C4RA05382F
- Liu, Y., Zou, J., Zeng, X., and Ding, W. (2015). Study on hydrogen storage properties of Mg-X (X = Fe, Co, V) nano-composites co-precipitated from solution. *RSC Adv.* 5, 7687–7696. doi: 10.1039/C4RA12977F
- Liu, Y., Zou, J., Zeng, X., Wu, X., Li, D., and Ding, W. (2014b). Hydrogen storage properties of a Mg-Ni nanocomposite coprecipitated from solution. *J. Phys. Chem. C* 118, 18401–18411. doi: 10.1021/jp504918x
- Lu, J., Choi, Y. J., Fang, Z. Z., Sohn, H. Y., and Rönnebro, E. (2010). Hydrogenation of nanocrystalline Mg at room temperature in the presence of TiH<sub>2</sub>. *J. Am. Chem. Soc.* 132, 6616–6617. doi: 10.1021/ja910944w
- Lukashev, R. V., Klyamkin, S. N., and Tarasov, B. P. (2006). Preparation and properties of hydrogen-storage composites in the MgH<sub>2</sub>-C system. *Inorg. Mater.* 42, 726–732. doi: 10.1134/S0020168506070077
- Ma, L. P., Kang, X. D., Dai, H. B., Liang, Y., Fang, Z. Z., Wang, P. J., et al. (2009). Superior catalytic effect of TiF<sub>3</sub> over TiCl<sub>3</sub> in improving the hydrogen sorption kinetics of MgH<sub>2</sub>: catalytic role of fluorine anion. *Acta Mater.* 57, 2250–2258. doi: 10.1016/j.actamat.2009.01.025
- Ma, T., Isobe, S., Wang, Y., Hashimoto, N., and Ohnuki, S. (2013). Nb-Gateway for hydrogen desorption in Nb<sub>2</sub>O<sub>5</sub> catalyzed MgH<sub>2</sub> nanocomposite. *J. Phys. Chem. C* 117, 10302–10307. doi: 10.1021/jp4021883

## AUTHOR CONTRIBUTIONS

The manuscript was written through contributions of all authors. All authors have given approval to the final version of the manuscript.

## FUNDING

This work was supported by the National Natural Science Foundation of China (51801100, 51771092, 21975125), Natural Science Foundation of the Jiangsu Higher Education Institutions of China (18KJB430014), Postgraduate Research & Practice Innovation Program of Jiangsu Province (SJCX18\_0341), Six Talent Peaks Project in Jiangsu Province (2018, XNY-020), and the Priority Academic Program Development (PAPD) of Jiangsu Higher Education Institutions.

- Norberg, N. S., Arthur, T. S., Fredrick, S. J., and Prieto, A. L. (2011). Size-dependent hydrogen storage properties of Mg nanocrystals prepared from solution. *J. Am. Chem. Soc.* 133, 10679–10681. doi: 10.1021/ja201791y
- Pistidda, C., Bergemann, N., Wurr, J., Rzeszutek, A., Möller, K. T., Hansen, B. R. S., et al. (2014). Hydrogen storage systems from waste Mg alloys. *J. Power Sources* 270, 554–563. doi: 10.1016/j.jpowsour.2014.07.129
- Ponthieu, M., Cuevas, F., Fernández, J. F., Laversenne, L., Porcher, F., and Lacroche, M. (2013). Structural properties and reversible deuterium loading of MgD<sub>2</sub>-TiD<sub>2</sub> nanocomposites. *J. Phys. Chem. C* 117, 18851–18862. doi: 10.1021/jp405803x
- Rather, S. U., Taimoor, A. A., Muhammad, A., Alhamed, Y. A., Zaman, S. F., and Ali, A. M. (2016). Kinetics of hydrogen adsorption on MgH<sub>2</sub>/CNT composite. *Mater. Res. Bull.* 77, 23–28. doi: 10.1016/j.materresbull.2016.01.025
- Rieke, R. D., and Hudnall, P. M. (1972). Activated metals. I. preparation of highly reactive magnesium metal. *J. Am. Chem. Soc.* 94, 7178–7179. doi: 10.1021/ja00775a066
- Rizo-Acosta, P., Cuevas, F., and Lacroche, M. (2018). Optimization of TiH<sub>2</sub> content for fast and efficient hydrogen cycling of MgH<sub>2</sub>-TiH<sub>2</sub> nanocomposites. *Int. J. Hydr. Energy* 43, 16774–16781. doi: 10.1016/j.ijhydene.2018.04.169
- Sander, J. M., Ismer, L., and Van De Walle, C. G. (2016). Point-defect kinetics in  $\alpha$ - and  $\gamma$ -MgH<sub>2</sub>. *Int. J. Hydr. Energy* 41, 5688–5692. doi: 10.1016/j.ijhydene.2016.01.156
- Schneemann, A., White, J. L., Kang, S., Jeong, S., Wan, L. F., Cho, E. S., et al. (2018). Nanostructured metal hydrides for hydrogen storage. *Chem. Rev.* 118, 10775–10839. doi: 10.1021/acs.chemrev.8b00313
- Shena, C., and Aguey-Zinsou, K.-F. (2017). Can  $\gamma$ -MgH<sub>2</sub> improve the hydrogen storage properties of magnesium? *J. Mater. Chem. A* 5, 8644–8652. doi: 10.1039/C7TA01724C
- Singh, R. K., Sadhasivam, T., Sheeja, G. I., Singh, P., and Srivastava, O. N. (2013). Effect of different sized CeO<sub>2</sub> nano particles on decomposition and hydrogen absorption kinetics of magnesium hydride. *Int. J. Hydr. Energy* 38, 6221–6225. doi: 10.1016/j.ijhydene.2012.12.060
- Siviero, G., Bello, V., Mattei, G., Mazzoldi, P., Battaglin, G., Bazzanella, N., et al. (2009). Structural evolution of Pd-capped Mg thin films under H<sub>2</sub> absorption and desorption cycles. *Int. J. Hydr. Energy* 34, 4817–4826. doi: 10.1016/j.ijhydene.2009.03.059
- Sun, Y., Ma, T., and Aguey-Zinsou, K.-F. (2018). Magnesium supported on nickel nanobelts for hydrogen storage: coupling nanosizing and catalysis. *ACS Appl. Nano Mater.* 1, 1272–1279. doi: 10.1021/acsnanm.8b00033
- Tang, F., Parker, T., Li, H. F., Wang, G. C., and Lu, T. M. (2008). The Pd catalyst effect on low temperature hydrogen desorption from hydrided ultrathin Mg nanoblades. *Nanotechnology* 19:465706. doi: 10.1088/0957-4484/19/46/465706
- Terent'ev, P. B., Gerasimov, E. G., Mushnikov, N. V., Uimin, M. A., Maikov, V. V., Gaviko, V. S., et al. (2015). Kinetics of hydrogen desorption from MgH<sub>2</sub> and AlH<sub>3</sub> hydrides. *Phys. Metals Metallogr.* 116, 1197–1202. doi: 10.1134/S0031918X15120121
- Vajeeston, P., Ravindran, P., Hauback, B. C., Fjellvåg, H., Kjekshus, A., Furuseth, S., et al. (2006). Structural stability and pressure-induced phase transitions in MgH<sub>2</sub>. *Phys. Rev. B* 73:224102. doi: 10.1103/PhysRevB.73.224102
- Varin, R. A., Czujko, T., and Wronski, Z. (2006). Particle size, grain size and gamma-MgH<sub>2</sub> effects on the desorption properties of nanocrystalline commercial magnesium hydride processed by controlled mechanical milling. *Nanotechnology* 17, 3856–3865. doi: 10.1088/0957-4484/17/15/041
- Wang, H., Hu, J., Han, F., Lu, Y., Liu, J., Ouyang, L., et al. (2015). Enhanced joint catalysis of YH<sub>2</sub>/Y<sub>2</sub>O<sub>3</sub> on dehydrogenation of MgH<sub>2</sub>. *J. Alloys Comp.* 645, S209–S212. doi: 10.1016/j.jallcom.2015.01.057
- Xiao, X., Liu, Z., Saremi-Yarahmadi, S., and Gregory, D. H. (2016). Facile preparation of  $\beta/\gamma$ -MgH(2) nanocomposites under mild conditions and pathways to rapid dehydrogenation. *Phys. Chem. Chem. Phys.* 18, 10492–10498. doi: 10.1039/C5CP07762A
- Yao, X., Zhu, Z. H., Cheng, H. M., and Lu, G. Q. (2011). Hydrogen diffusion and effect of grain size on hydrogenation kinetics in magnesium hydrides. *J. Mater. Res.* 23, 336–340. doi: 10.1557/JMR.2008.0063
- Yartys, V. A., Lototsky, M. V., Akiba, E., Albert, R., Antonov, V. E., Ares, J. R., et al. (2019). Magnesium based materials for hydrogen based energy storage: past, present and future. *Int. J. Hydr. Energy* 44, 7809–7859. doi: 10.1016/j.ijhydene.2018.12.212
- Zaluska, L., Zaluska, A., Tessiera, P., Ström-Olsena, J. O., and Schulz, R. (1995). Catalytic effect of Pd on hydrogen absorption in mechanically alloyed Mg<sub>2</sub>Ni, LaNi<sub>5</sub> and FeTi. *J. Alloys Comp.* 217, 295–300. doi: 10.1016/0925-8388(94)01358-6
- Zhang, X., Leng, Z., Gao, M., Hu, J., Du, F., Yao, J., et al. (2018). Enhanced hydrogen storage properties of MgH<sub>2</sub> catalyzed with carbon-supported nanocrystalline TiO<sub>2</sub>. *J. Power Sources* 398, 183–192. doi: 10.1016/j.jpowsour.2018.07.072
- Zhang, Y., Zhuang, X., Zhu, Y., Wan, N., Li, L., and Dong, J. (2015). Synergistic effects of TiH<sub>2</sub> and Pd on hydrogen desorption performances of MgH<sub>2</sub>. *Int. J. Hydr. Energy* 40, 16338–16346. doi: 10.1016/j.ijhydene.2015.09.029
- Zhou, S., Ran, W., Yang, M., Wang, D., Chen, G., Zhang, Y., et al. (2013). Magnesium hydride of orthorhombic crystal from high-energy ball milling under hydrogen atmosphere. *Adv. Mater. Res.* 724–725, 1033–1036. doi: 10.4028/www.scientific.net/AMR.724-725.1033
- Zhou, S., Zhang, Q., Chen, H., Zang, X., Zhou, X., Wang, R., et al. (2015). Crystalline structure, energy calculation and dehydrating thermodynamics of magnesium hydride from reactive milling. *Int. J. Hydr. Energy* 40, 11484–11490. doi: 10.1016/j.ijhydene.2015.02.059

**Conflict of Interest:** The authors declare that the research was conducted in the absence of any commercial or financial relationships that could be construed as a potential conflict of interest.

Copyright © 2020 Liu, Zhu, Liu, Zhu, Zhang and Li. This is an open-access article distributed under the terms of the Creative Commons Attribution License (CC BY). The use, distribution or reproduction in other forums is permitted, provided the original author(s) and the copyright owner(s) are credited and that the original publication in this journal is cited, in accordance with accepted academic practice. No use, distribution or reproduction is permitted which does not comply with these terms.